CHALMERS
UNIVERSITY OF TECHNOLOGY

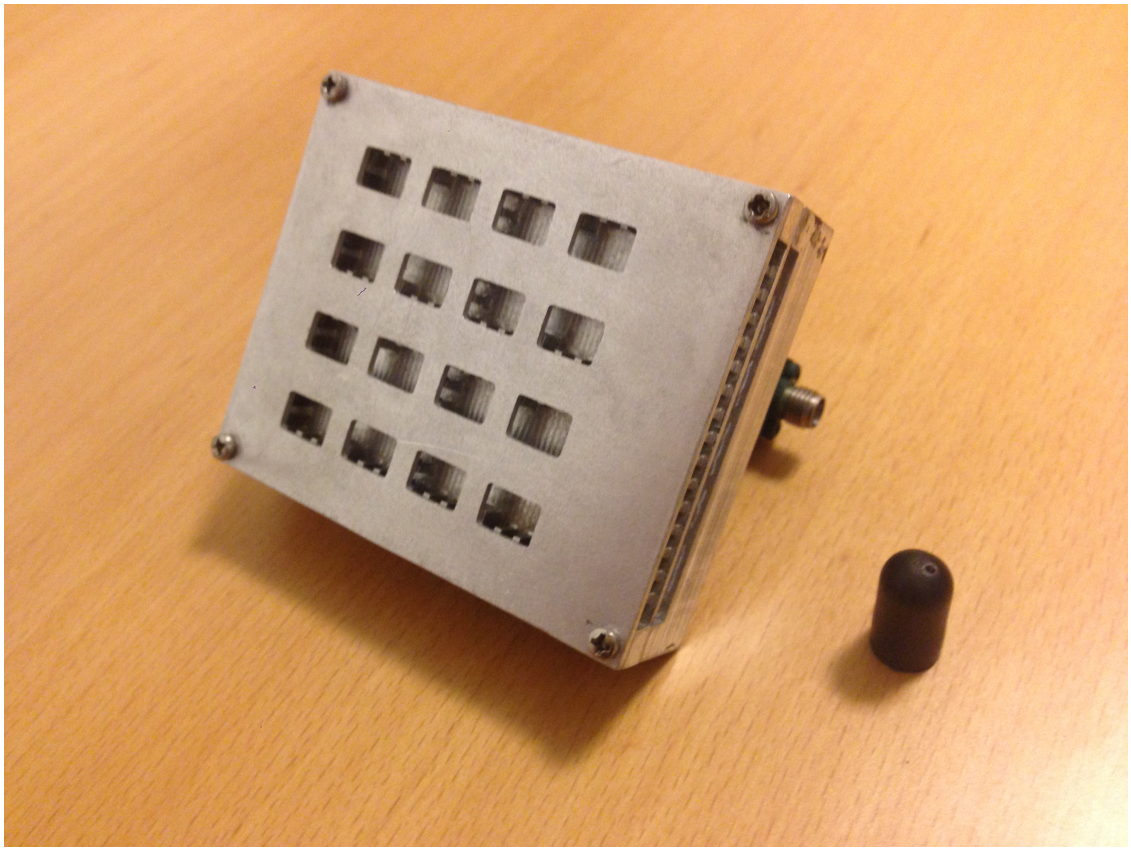

Design of a Double Layer Cavity backed Slot Array Antenna in Gap Waveguide Technology

PEIYE LIU

Department of Signals and Systems
CHALMERS UNIVERSITY OF TECHNOLOGY
Gothenburg, Sweden 2016

Master's thesis 2016:NN

Design of a Double Layer Cavity backed Slot Array Antenna in Gap Waveguide Technology

PEIYE LIU

CHALMERS
UNIVERSITY OF TECHNOLOGY

Department of Signals and Systems
Antenna group
Chalmers University of Technology
Gothenburg, Sweden 2016

Design of a Double Layer Cavity backed Slot Array Antenna in Gap Waveguide Technology

PEIYE LIU

Supervisor: Assistant Professor Ashraf Uz Zaman
Examiner: Professor Per-Simon Kildal

Master's Thesis 2016:NN
Department of Signals and Systems
Antenna Group
Chalmers University of Technology
SE-412 96 Gothenburg
Telephone +46 31 772 1000

Printed in by Chalmers University of Technology
Gothenburg, Sweden 2016

Design of a double layer cavity backed Slot Array Antenna design in Gap waveguide technology
PEIYE LIU
Department of Signals and Systems
Chalmers University of Technology

Abstract

This thesis presents the design of a double layer cavity backed slot array antenna at K-band in gap waveguide technology. Gap waveguide technology is a solution to reduce the performance gap between planar transmission lines and metal waveguide in terns of loss, manufacturing flexibility and cost. And it could also solve the packaging problems of microwave electronic circuit.

The antenna was designed in two layers separately using CST microwave studio. Optimizations were done towards minimized reflection coefficient ,maximized gain, high efficiency and wide bandwidth. The simulated impedance bandwidth is 20% for a 4×4 element array antenna. A test antenna is fabricated and tested, reflection coefficient remains below -11dB with reasonably good radiation patterns over the band of interest.

Keywords: Double layer, slot array, gap waveguide technology, wide band, high efficiency.

Acknowledgements

First of all I would like to thank my examiner Professor Per-Simon Kildal, for giving me this opportunity to work in Antenna group. I would also thank my supervisor assistant professor Ashraf Uz Zaman who have been supportive during the whole period and gave me lots of advices with great patient.

Also I would like to thank all members in the antenna group at Chalmers for creating an enjoyable working environment. They created a good atmosphere which keeps me positive and away from too much pressure.

In the end, I would like to thank my family for their support and encouragement throughout these years. Without you, I could never make this far.

Peiye Liu
Gothenburg, 2016

Contents

1

Introduction

In recent years, there is a significant growth of RF components, circuits and antennas designed in millimeter wave or even higher frequency spectrum . These antennas are mostly fed by metal waveguide or planar transmission lines. However conventional feed network technologies have critical problems. And even at low frequency, these disadvantages can not be neglected.

1.1 Planar Transmission Line Problems

Microstrip and coplanar lines are two commonly used planar transmission lines. These are robust, low cost and very suitable for integrating active microwave components. But they both suffer from high insertion loss and significant power leakage at high frequency[1, 2]. Another problem is that these lines has high width to wavelength ratio, at high frequencies, it brings unwanted substrate mode and surface current, then causes unexpected cross-talk, isolation and packaging problems[3].

An example in study[4], 4×4 patch antennas and arrays on LTCC with embedded-cavity substrates achieved a maximum gain of 18.2dBi over 57-64GHz frequency band, see Fig 1.1.

Figure 1.1: 4×4 patch antennas and arrays (a) Radiating patches, (b) Reactive feed network, and (c) Wilkinson feed network[4].

1.2 Metal Waveguide Problems

On the other hand, metal waveguide has quite low loss and are very suitable for low loss and high Q components[5, 6]. And in antenna design, it could achieve high radiation efficiency. However, the strict requirement of surface contact at high frequency make it costly and complex to manufacture.

A common rectangular waveguide is shown in Fig 1.2, its E-field strength is maximum at the center of E-plane and zero at inner wall surface. In contrast, its H-field strength reaches maximum at inner wall surface. If manufactured by the method show in Fig 1.3(right), without very good surface contact, this will result in significant leakage in these splits.

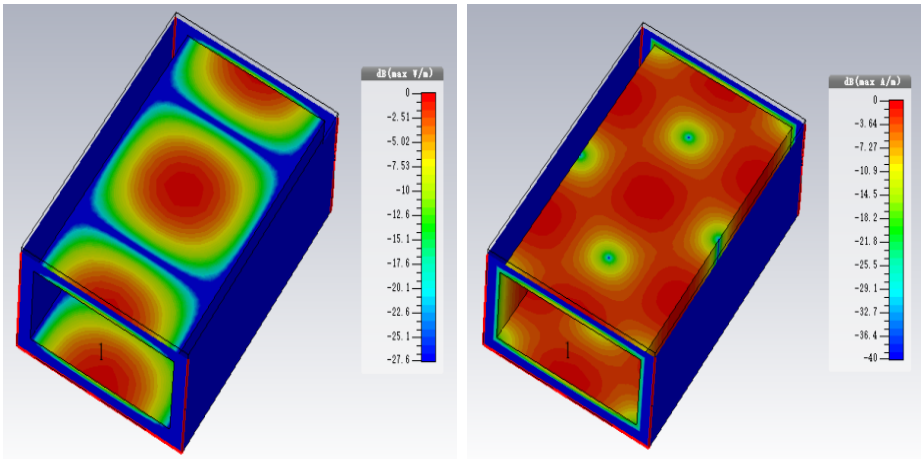

Figure 1.2: Standard rectangular waveguide: E-field(mid) H-field and surface current(right).

As in [7], a 16×16 slot antenna array fed by an amplitude-tapering waveguide feed network is designed. It achieved 13.8% bandwidth and gain of more than 29.5dBi at Ku band using traditional fabrication method shown in 1.3(right). While theoretically a 16×16 slot array antenna could have a gain of 32-33dBi. The 3dB performance gap is due to the leakage. Although example shown in Fig1.4 [8] overcome leakage problem, but its cost is quite expensive and hard to integrate MMIC or RF components.

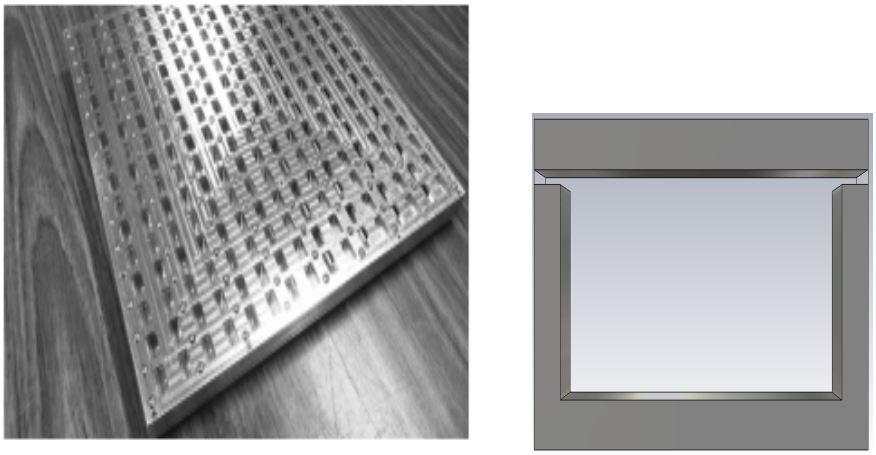

Figure 1.3: Prototype of 16×16 slot antenna array fed by rectangular waveguide and its fabricating method sketch map[7].

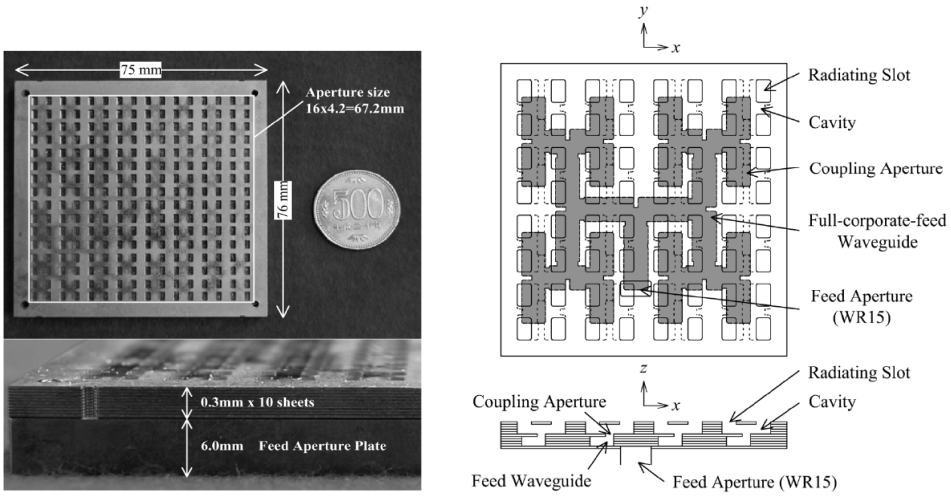

Figure 1.4: 16×16 slot array antenna fed by rectangular waveguide at 60GHz band: Fabricated antenna(left), Configuration(right)[8].

Another way to assemble rectangular waveguide is introduced in [9], as show in Fig 1.5(right). Instead, waveguide is cut at the center of E-field which could avoid leakage through splits. But with this method, a whole component will be divided into too great parts when manufacturing as shown in Fig 1.5 which increases the cost to some extent.

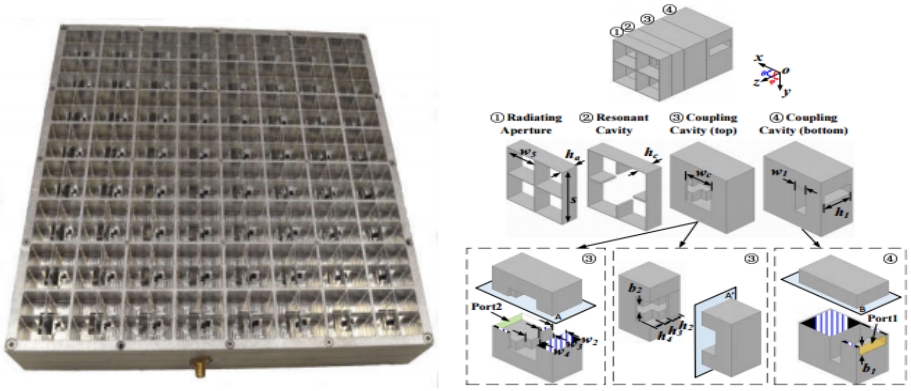

Figure 1.5: Prototype of the 16 × 16 dual-polarization antenna array and Configuration of the 2 × 2-element sub-array[9].

1.3 Brief Overview of the Thesis

To narrow down the performance gap in terms of loss, manufacturing flexibility and cost between the planar transmission lines and metal waveguide, gap waveguide technology was proposed[8]-[11]. In this thesis, a double layer cavity backed slot array antenna using gap waveguide technology has been designed, manufactured and tested shown in Fig 1.6.

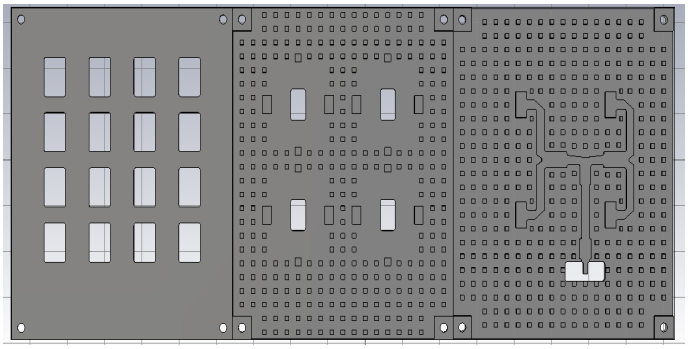

Figure 1.6: K band double layer cavity backed slot array antenna.

Other chapters of this thesis are shown below

Chapter 2 Discussed the basic principle of gap waveguide technology. Its main advantages and some presents works have been discussed and shown in this chapter.

Chapter 3 Describes the design of slot array and its back cavity. The unit cell consist of a 2 × 2 element slot array and its back cavity fed by a small parts of feed network. Far field pattern along with reflection efficiency(S_{11}) will be analysed with open boundary on top surface and periodic boundary at four horizontal surfaces.

Chapter 4 Describes the design of the complete antenna. Feed network(bottom layer) is discussed by two parts: T-junction power divider, and transition from rect-

angular waveguide to ridge gap waveguide. Then a combination of these parts is fed by a standard waveguide WR-42(K band), and its S_{11} is analysed with periodic boundary using CST microwave studio. At the end of this chapter, these layers have been combined together into the complete antenna.

Chapter 5 Shows the manufactured prototype and measurement results. And the performance gap between results of prototype tested and that of simulated have been discussed.

Chapter 6 Conclusion of the thesis.

2

Overview of Gap Waveguide Technology

To overcome the problems mentioned in chapter one, gap waveguide technology was proposed in 2009[10]-[16]. This technology is comparably low loss, flexible in manufacturing which could be a solution to reduce the performance gap between planar transmission lines and metal waveguide[10]-[14].

Four different types of gap waveguide are shown in Fig 2.1.

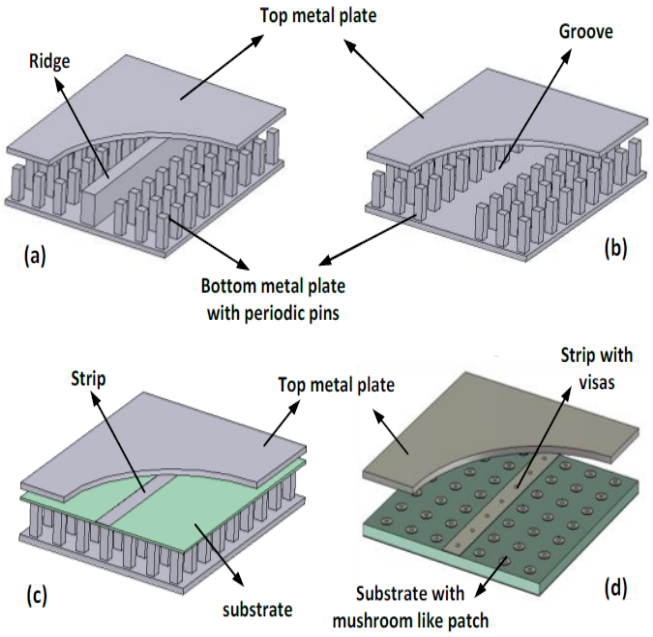

Figure 2.1: Different gap waveguide geometries: a) Ridge gap waveguide, b) Groove gap waveguide, c) Inverted- microstrip gap waveguide, d) Microstrip-ridge gap waveguide[17].

2.1 Basic Principle of Gap Waveguide Technology

Gap waveguide technology is based on the idea of soft and hard surfaces. It is basically a combination of a Perfect Electric Conductor(PEC) plane and a Perfect

Magnetic Conductor(PMC) plane paralleled with an air gap smaller than a quarter wavelength in between as shown in Fig 2.2.[10]-[15]

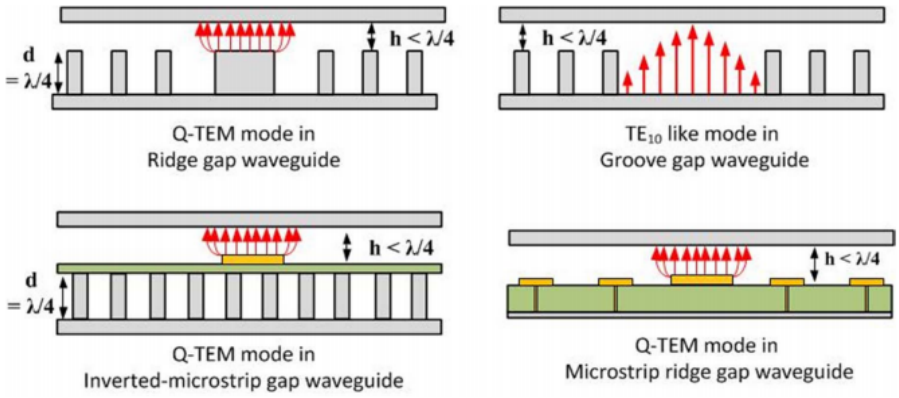

Figure 2.2: Mode in four types of gap waveguide[17].

The air gap between PEC and PMC surfaces create a cut-off condition to stop electromagnetic wave from propagation. Then if there exist a ridge, groove or microstrip line in the PMC plane, EM wave will only propagate along them without leakage in any other directions.

Table 2.1: Comparisons of insertion loss results of different gap waveguide structures at V band[17].

	Simulated maximum loss(dB/cm)	Measured minimum loss(dB/cm)	Measured maximum loss(dB/cm)
Rectangular waveguide(extruded)	0.0134	0.022	0.042
Rectangular waveguide (E plane split blocks)	0.01355	0.024	0.046
Groove gap waveguide	0.019	0.026	0.045
Ridge gap waveguide	0.05	0.053	0.073
Microstrip-ridge gap waveguide	0.0805	0.18	0.22
Inverted- microstrip gap waveguide	0.093	0.21	0.27
Normal Microstrip line(0.127mm subst.)	0.37	0.63	0.77

With an air gap between two surfaces, there is no need for electrical contact which solved the problem of good electric contact between the metal layers. And according to Table 1.1, gap waveguide has much less loss compared with normal microstrip

line and losses are similar to conventional rectangular waveguide.

Also the gap waveguide technology is very suitable for RF packaging[18]-[20], which plays am important role in integrating RF electronics with antenna, and has high radiation efficiency in antenna design like metal waveguide.

2.2 Components using Gap Waveguide Technology

In recent years, several components such as filter and antenna at different frequency range have been designed based on gap waveguide technology and it will play a important role in future passive components design, as shown below: V band groove gap waveguide duplexer in Fig 2.3[21, 22], Ku band linear slot array in ridge gap waveguide in Fig 2.4[23] and Ku band high-Q groove gap waveguide third- and fifth-order filter in Fig 2.5[24].

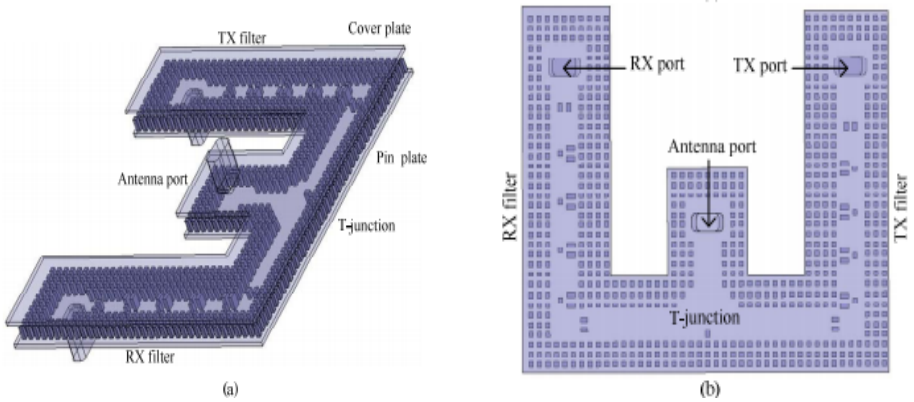

Figure 2.3: V band groove gap waveguide duplexer. (a) 3D view and (b) top view[21, 22].

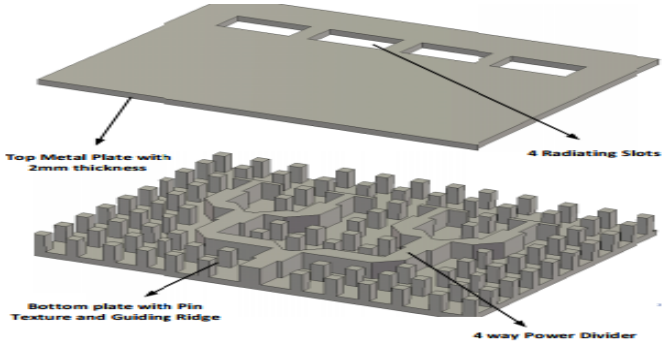

Figure 2.4: Ku band linear slot array in ridge gap waveguide[23].

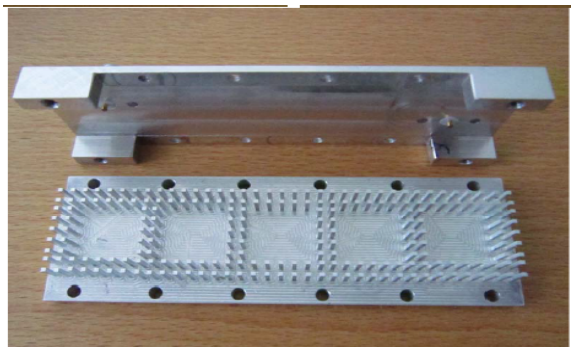

Figure 2.5: Ku bandh high-Q groove gap waveguide fifth-order filter[24].

3

Antenna Unit Cell Design

In this chapter , a 2×2 elements sub-array unit cell has been designed. Fig 3.1 shows exploded perspective view of unit cell. It consist of several layers. Top most is radiating slots. The cavity below is partitioned into four parts by two sets of metal blocks, and the coupling slot is placed at the center of the cavity. In lower layer a T-section is placed to feed the cavities. The 2×2 elements sub-array is excited with same amplitude and phase. All results are simulated using CST.

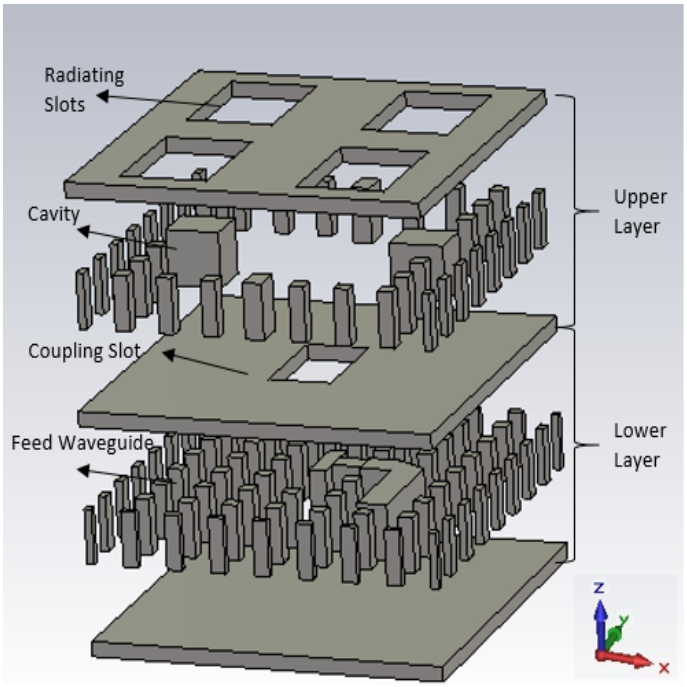

Figure 3.1: Exploded perspective view of 2×2 elements sub-array unit cell.

3.1 Stop Band Design

As mentioned in chapter two, to create a stop band, we need to design a bed of periodic pins which acts like PMC surface. Shown in Fig 3.2 is side view of rows of pins and its dispersion diagram. We could see that there is no electromagnetic wave propagation between 15GHz and 37GHz. Simulation is done using eigen mode.

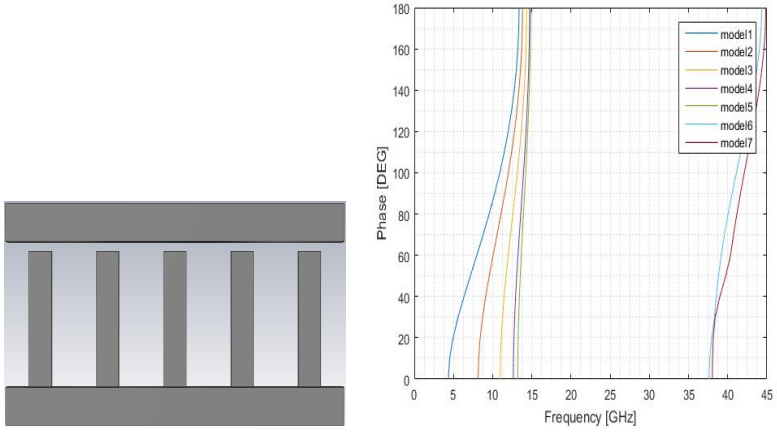

Figure 3.2: Bed of Pins and Dispersion Diagram.

This is the basic structure of the gap waveguide used in the entire design. Stop band is designed based on study in [25]-[27]. Dimension of Pin is $1 \times 1mm^2$ with height of 3.6mm and period of 3mm, air gap is kept 0.25mm.

3.2 Single Slot Design

As previously studied in [23], an additional added T-section could improve the bandwidth. In order to realize the strong excitation of cavity, it has an offset from the center axis of the coupling slot. Exploded view of the T-section is shown in Fig 3.3.

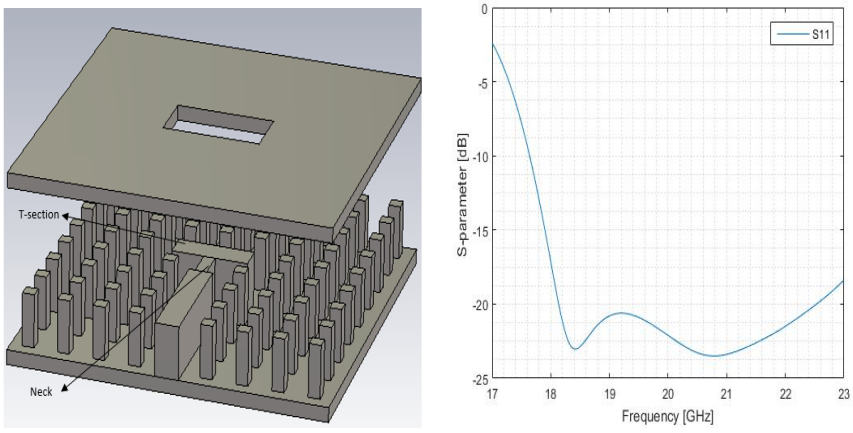

Figure 3.3: Exploded view of the T-section and its Simulation result[23].

Results are simulated using periodic boundary walls in two sides and open boundary on top. S_{11} is below -20dB over the range from 18.1GHz to 22.9GHz. Selected parameters are shown in Table 3.1.

Table 3.1: Values in T-section.

Symbol	Description	*Value*
cpl	length of coupling slot	8.39mm
cpw	width of coupling slot	4.52mm
offset_ts	offset distance of T-section	0.91mm
tsl	length of T-section	6.45mm
tsw	width of T-section	2.03mm
tw	width of neck	0.97mm
twl	length of neck	1.98mm

3.3 Double Layer Concept

Fig 3.4 shows the slot coupling mechanism of the unit cell. The magnetic field of the TEM mode in the feed network has mainly the y component at the coupling aperture. The magnetic field in the cavity becomes symmetrical distribution with respect to the x direction[8].

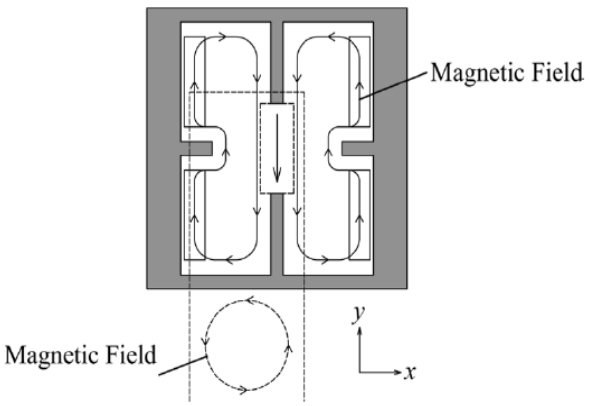

Figure 3.4: Slot coupling mechanism[8].

Two sets of periodic boundary are placed in the external region to simulate the mutual coupling in the infinite two-dimensional slot array. Boundary on top and bottom are open and PEC, respectively. Two sets of metal blocks are placed to suppress unwanted higher modes in the cavity. The key factor of the design is to ensure that the magnetic field pass through the center of four radiating slots and coupling slot.

3.4 Sub-array Unit Cell Design

The design frequency of the antenna is around 20GGHz and the slot spacing in both x and y direction are chosen to be 12mm to simplify the structure building when

using same pin period in lower layer. On the top layer, the element spacing is kept 0.82λ.

According to studies in [23], dimensions of the of T-section and coupling slot are key parameters which affect the results while dimensions of the neck have relatively smaller effect. In the unit cell design, the neck is deleted to simplify manufacturing.

In simulation, first set of parameters need to be decided is dimensions of radiating slot, according to former study in [8] ratio of w/l is related to bandwidth. Then varying the dimensions of two sets of metal blocks together with coupling slot to achieve a better directivity. Finally T-section is matched with top layer to get low refection in desired bandwidth.

Simulation results are shown below.

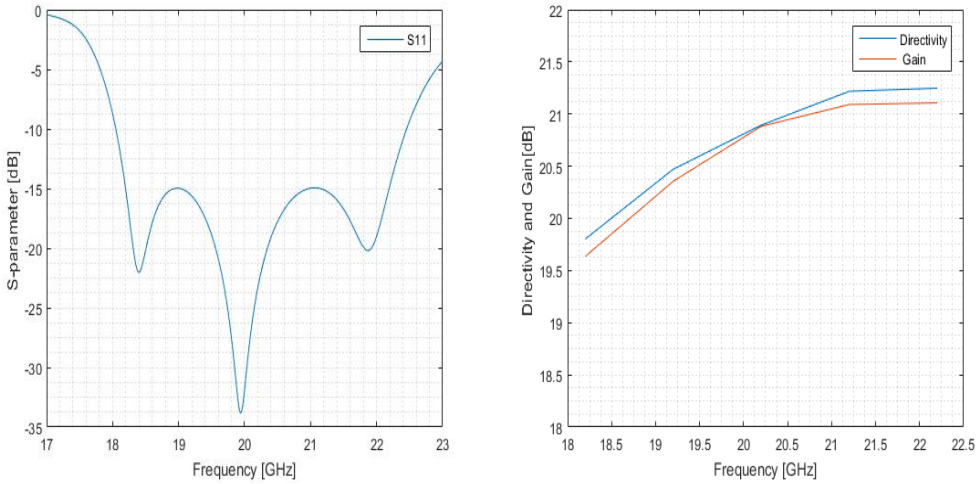

Figure 3.5: Simulated results of unit cell.

From figures above, we could see S_{11} is -15dB from 18.2GHz to 22.2GHz corresponding to a 19.8% bandwidth. Directivity is about 15 dBi, aperture efficiency is above 95% over the whole frequency range.

Further more, radiation pattern of 2×2 array unit cell is shown in Fig 3.6, which correspond to the ones of complete antenna.

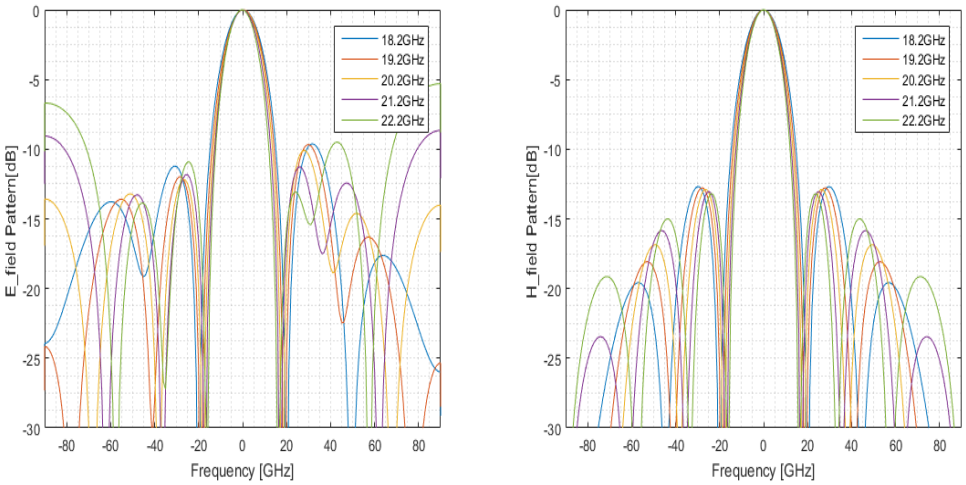

Figure 3.6: E-(left) and H-field(right) pattern at different frequency of 2×2 array.

All parameters are listed in Table 3.2.

Table 3.2: Values of 4×4 slot array.

Symbol	Description	*Value*
sl	length of slot	8.52mm
sw	width of slot	5.77mm
cpl	length of coupling slot	7.41mm
cpw	width of coupling slot	4.26mm
offset_ts	offset distance of T-section	0.92mm
tsl	length of T-section	6.8mm
tsw	width of T-section	2.85mm
xl	length of x-axis ridge	2.54mm
xw	width of x-axis ridge	3.7mm
yl	length of y-axis ridge	2.1mm
yw	width of y-axis ridge	1.43mm

3.5 60GHz Unit Cell

To check gap waveguide performance at high frequency, the unit cell was further scale by factor of 1/3. Then a new unit cell working at 60GHz was obtained. With all boundaries the same, optimized results are shown below.

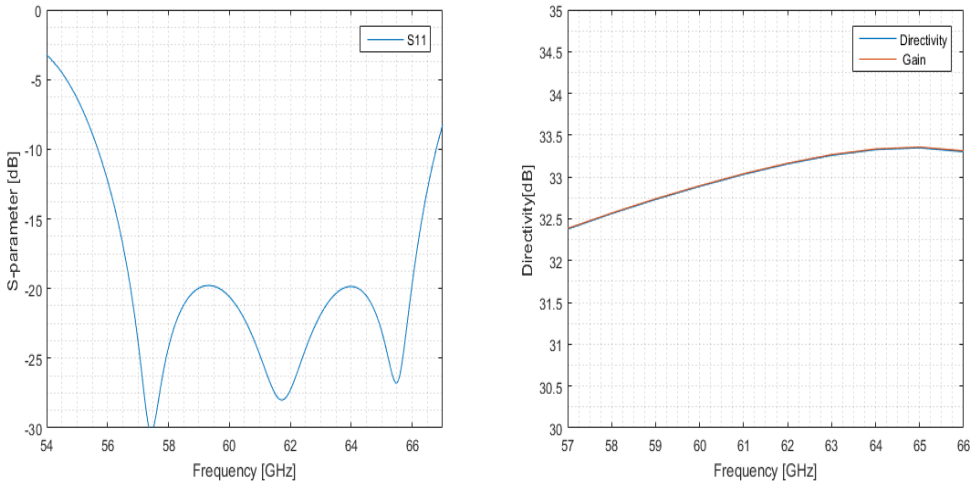

Figure 3.7: Optimized results of 60GHz 16×16 elements array.

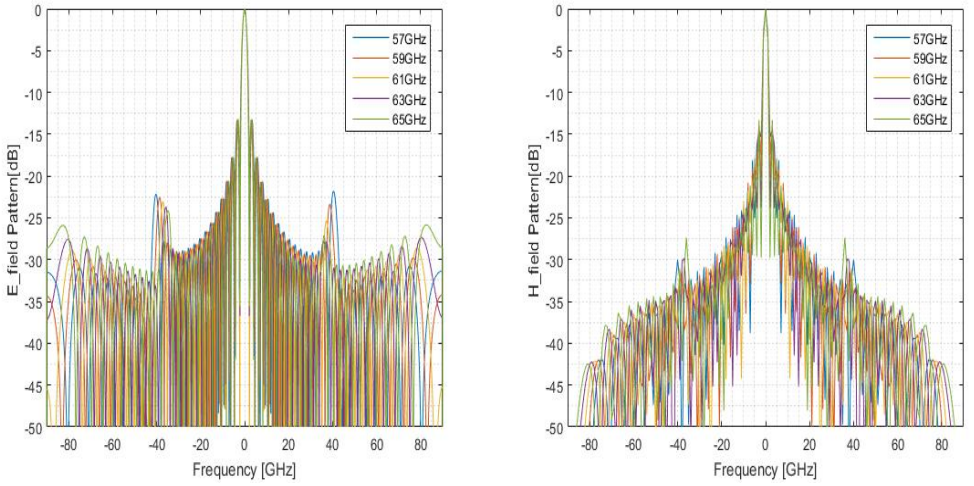

Figure 3.8: E-(left) and H-field(right) pattern at different frequency optimized 16×16 elements array.

Then, we get a bandwidth with reflection of -20dB of 15%(57 - 66GHZ) for a 16×16 element array. Parameters obtained are listed in Table 3.3.

Table 3.3: Values of 16 × 16 slot array.

Symbol	Description	*Value*
sl	length of slot	2.82mm
sw	width of slot	1.9mm
cpl	length of coupling slot	3.28mm
cpw	width of coupling slot	0.94mm
tsl	length of T-section	3.52m
tsw	width of T-section	1mm
xl	length of x-axis ridge	0.56mm
xw	width of x-axis ridge	2.05mm
yl	length of y-axis ridge	0.51mm
yw	width of y-axis ridge	0.7mm

3.6 Summary

This chapter describes the design of unit cell at 20GHz and scaled one at 60GHz. These designs all consist T-section which is a part of feed network to make impedance match. Reflection loss of unit cell at 20GHz is -15dB with 20% bandwidth, and aperture efficiency is over 95%.

4

Complete Antenna Design

In this chapter, a complete feed network has been designed using ridge gap waveguide technology. Shown in Fig 4.1 is the top view of feed network. It's excited by a waveguide port the same size as WR-42(K band) at the bottom, then through two T-junction power dividers EM wave is equally divided and redirected into four branches. Four coupling slots are covered by waveguide ports to examine phase imbalance and insertion loss.

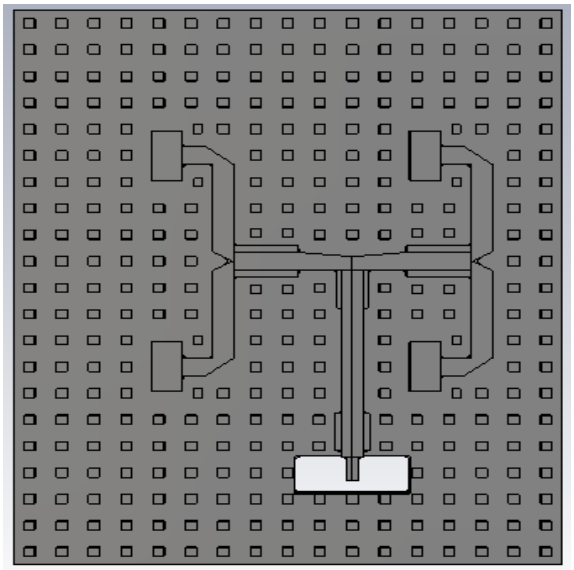

Figure 4.1: Top view of feed network.

The feed network is designed and optimized by each part: transition from wr-42 to ridge gap waveguide, T-junction power diveder, then these parts are combined together to check its performance. Stop band used in feed network is the same in unit cell.

4.1 Transition from WR-42 to Ridge Gap Waveguide

To simplify the design, the parameters should be reduced as much as possible. Here a hollow waveguide excited from bottom is used in simulation, its dimensions are

$10.7 \times 4.3mm^2$ according to standard WR-42.

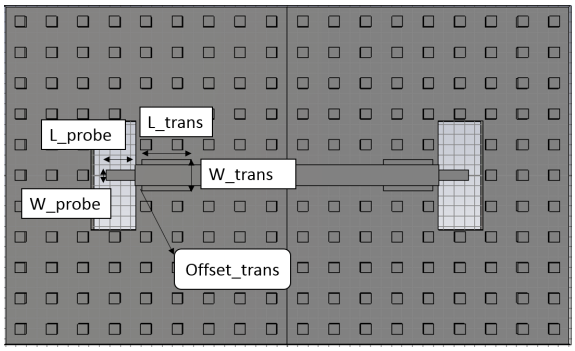

Figure 4.2: Top view of WR-42 to ridge gap waveguide transition[28].

Fig 4.2 is a back to back geometry of WR-42 to ridge gap waveguide transition. To achieve good impedance matching and without causing too much manufacturing complexity, a three step transformer has been used to match the impedance. As pin size and its period are all set in chapter two, and width of the ridge is chosen to be 2mm, the parameters remained which can influence the transition design are dimensions of the rectangular probe(width W_probe and length L_probe), dimensions of transformer(width W_trans and length L_trans) and its position(Offset_trans).

Keeping stop band the same, then varying the parameters mentioned above to get a good return loss around 20GHz. The final simulated result is shown in Fig 4.3.

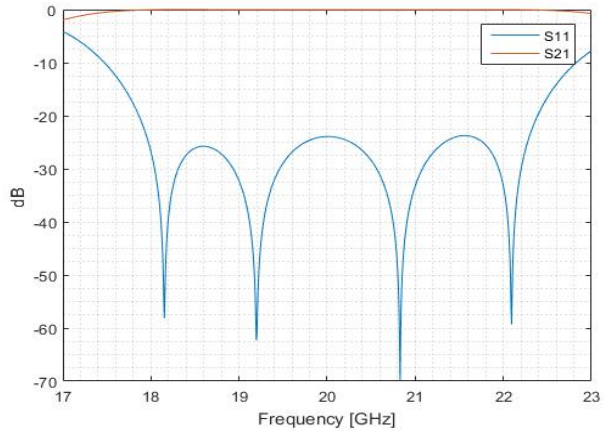

Figure 4.3: Simulated results for WR-42 to ridge gap waveguide transition.

Return loss(S_{11}) is below -22dB over 18GHz to 22.2GHz, and insertion loss is quite low at the same frequency range. All paremeters are shown in Table 4.1.

Table 4.1: Values in WR-ridge.

Symbol	Description	*Value*
b_angle	angle of bend	45.5°
b_w	width of bend	2.08mm
L_probe	length of probe	2.67mm
W_probe	width of probe	0.79mm
Offset_trans	offset distance of WR-ridge transformer	0.63mm

4.2 Design of T-junction Power Divider

To feed a 4×4 element slot array antenna with cavity back, two level of T-junction power divider are needed. The input power need to be delivered into four branches with same amplitude and phase. Top view of single T-junction power divider is shown in Fig 4.4. EM wave propagate through feed ridge to transformer, then into two branches.

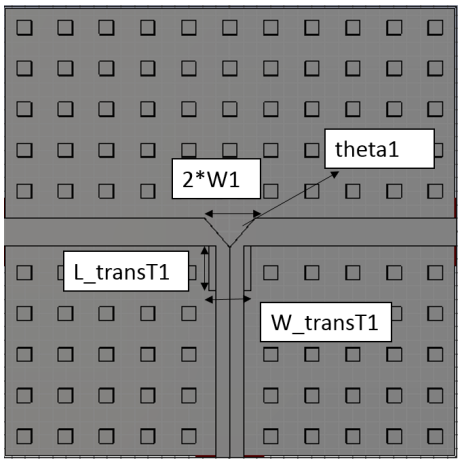

Figure 4.4: Top view of single T-junction power divider[28].

The first thought here is using a quarter wave transformer, but due to the space limitation and the difficulties of precisely calculation for ridge gap waveguide's impedance, quarter wave transformer was abandoned. Another way to make impedance match is using tapered lines which can avoid the limitation of small space in gap waveguide. Simulation results are shown in Fig 4.5.

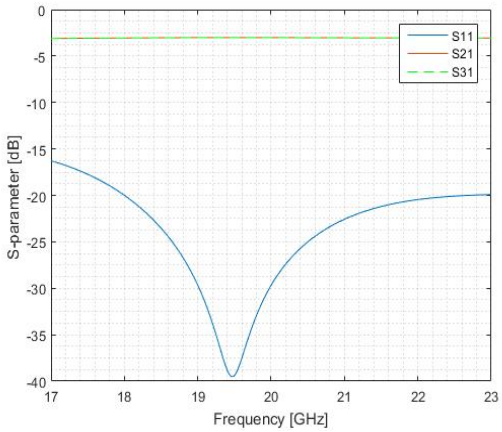

Figure 4.5: Simulation results of single T-junction.

S_{11} is below -20dB over the range from 18GHz to 22GHz. S_{21}/S_{31} are -3dB over the whole frequency range indicating that they are with the same amplitude. All parameters are shown in Table 4.2
.

Table 4.2: Values in single T-junction.

Symbol	Description	*Value*
L_transT1	length of first Tjunction transformer	3.27mm
W_transT1	width of first Tjunction transformer	3.12mm
W1	Width of first T-junction compensation bend	2.151mm
theta1	angle of first T-junction compensation bend	40.4°

Then the single T-structure was used to designed to be four way power divider as shown in Fig4.6. Double T-junction power divider uses the same parameter as single T-junction power divider. One port is placed at the end of each branch.

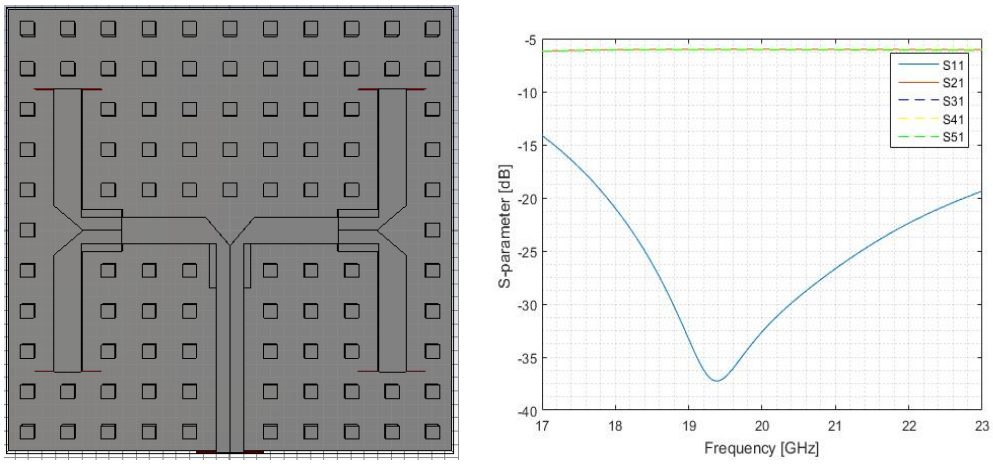

Figure 4.6: Top view and simulation result of double T-junction power divider.

Simulation results are shown in Fig 4.6 right, S_{11} is still below -20dB over the range from 18GHz to 22.5GHz. The bandwidth is improved. $S_{21}/S_{31}/S_{41}/S_{51}$ are almost -6.15dB over the whole range with only a slight(0.03dB) difference at low and high frequency which could be neglected.

Finally, to feed the unit cell designed in chapter two and make sure all output port signal are in phase, bend is added at end of branch with same parameters in double T-junctions shown in Fig 4.7.

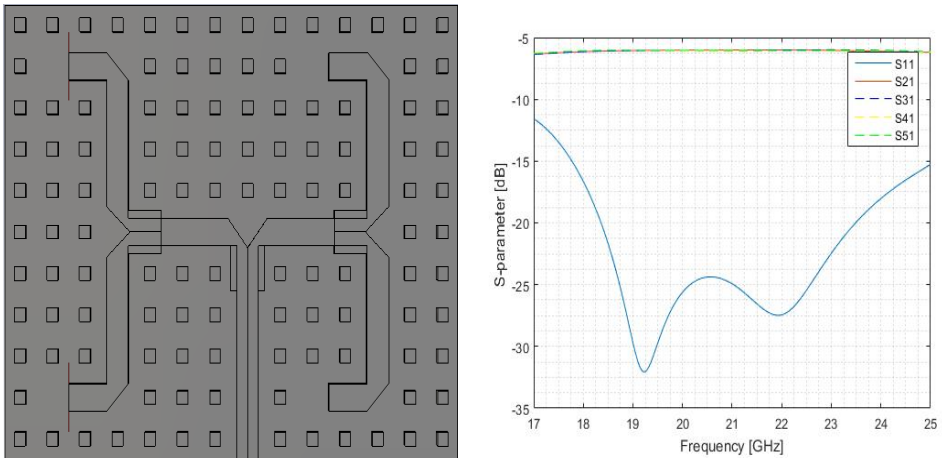

Figure 4.7: Top view of double T-junction power divider with bend and simulation results.

Simulation results are shown in Fig 4.7, the varied parameters are bend_angle and bend_width. We could see from the figure, S_{11} is worse, bandwidth moved a bit towards high frequency. That is simply because bend brings correspondingly large reflection. But still a bandwidth of 25% with S_{11} below -20dB is achieved. Band_width and Band_angle are 45° and 2mm respectively.

4.3 Combined Feed network

After combining WR-42 to ridge and double T-junction with bend together, we get a full corporate feed network and its performance is optimized and shown in Fig 4.8.

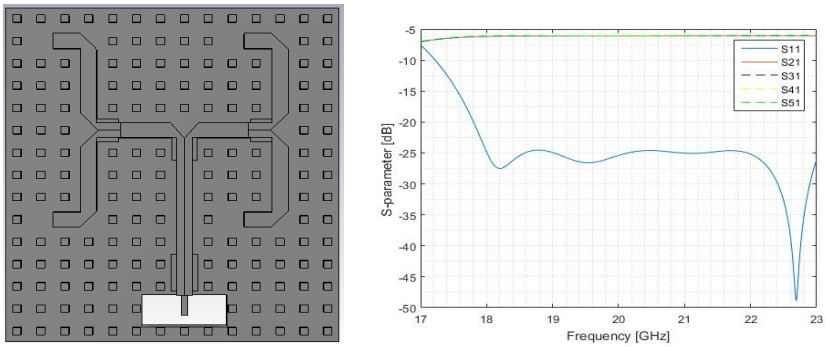

Figure 4.8: Full corporate feed network and its simulated results.

From the results we could see that S_{11} is about -25dB from 18GHz to 23GHz and quite smooth, and $S_{21}/S_{31}/S_{41}/S_{51}$ are around -6.15dB with not much difference that indicate four output ports are in same amplitude and insertion loss(-0.15dB) is acceptable.

All parameters selected are shown in Table 4.3.

Table 4.3: Values in full corporate feed network

Symbol	Description	*Value*
a	width of ridge	2mm
b_angle	angle of bend	45.5°
b_w	width of bend	2.08mm
L_probe	length of probe	2.67mm
W_probe	width of probe	0.79mm
Offset_trans	offset distance of WR-ridge transformer	0.63mm
L_trans	length of WR-ridge transformer	4.9mm
W_trans	width of WR-ridge transformer	3.21mm
L_transT1	length of first Tjunction transformer	3.05mm
W_transT1	width of first Tjunction transformer	3.21mm
L_transT2	length of second Tjunction transformer	3.05mm
W_transT2	width of second Tjunction transformer	3.17mm
W1	Width of first T-junction compensation bend	2.08mm
theta1	angle of first T-junction compensation bend	40.2°
W2	Width of second T-junction compensation bend	2.2mm
theta2	angle of second T-junction compensation bend	45.7°

4.4 Complete Antenna

The prototype is designed by combining two parts that former designed together. Four unit cell in upper layer is placed as 4×4 array which could be fed by four branches in lower layer in same amplitude and phase. Its exploded view is shown in Fig 1.6.

The prototype needs to be optimized due to the feed network does not match with upper cavities as they were optimized separately. Here only parameters in feed networks are varied because radiation patterns we got from unit cell are good. Optimized results are shown in Fig 4.9.

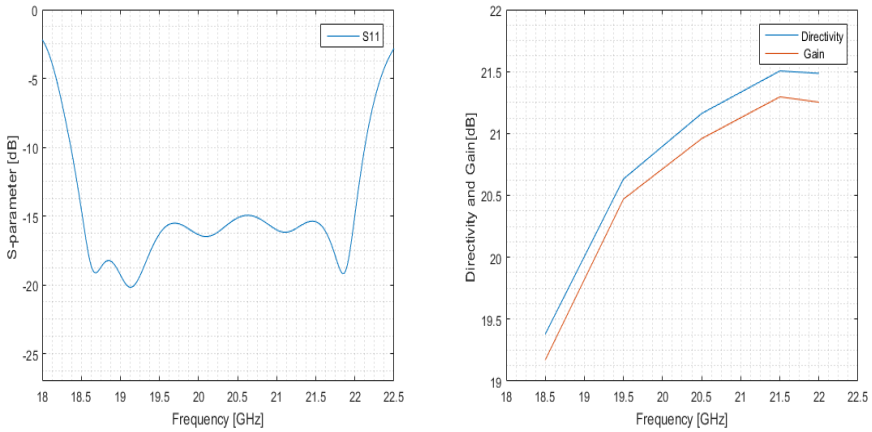

Figure 4.9: First optimized results of prototype.

Reflection loss is -15dB which is good, but bandwidth is not as wide as expected. Then we further vary parameters in upper layer slightly to try to get a better bandwidth while not affect radiation pattern much. Final optimized results are shown in figure below.

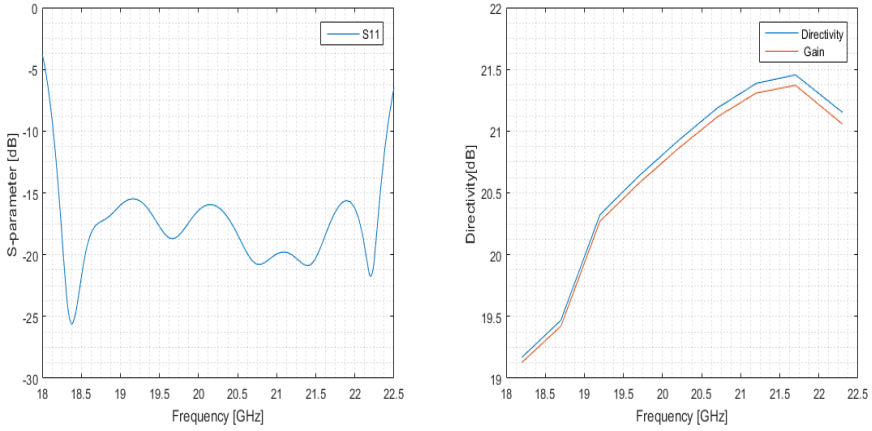

Figure 4.10: Final optimized results of prototype.

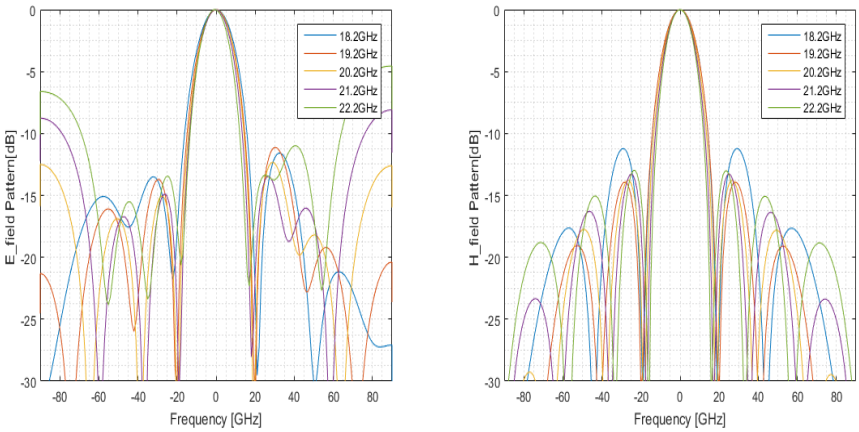

Figure 4.11: Final E-(left) and H-field(right) pattern of prototype.

This time we get a bandwidth of 20% with reflection loss -15dB. Directivity are quite agreed with ones calculated, although at high frequency it decreased by 1dB.

4.5 Summary

The design of feed network and complete antenna has been described in this chapter. By connecting a WR-42 at bottom, bottom layer can feed a 4×4 slot array with same amplitude and same phase. Reflection loss is -25dB over the desired band which is acceptable low and quite smooth. The prototype of the complete antenna achieved a bandwidth of 20% with reflection loss -15dB. and directivity are quite agreed with the one calculated.

5

Test and Measured Results

In this chapter, the prototype of complete antenna is re-designed, manufactured and tested. For manufacturing, additional rows of pins and standard flange holes have been added. Then reflection coefficient and far-field radiation pattern have been measured in anechoic chamber.

5.1 Re-Design of Prototype

The prototype was re-designed to comply with manufacturing. Two rows of pins have been added at x and y axis boundaries in both upper and lower layers to make enough space for screw holes. At bottom four more screw holes were made for standard flange. All sharp corners in former design including ones in hollow waveguide at bottom are changed into round ones with radius of 0.5mm. While manufacture method used is milling, there is a limitation of drill size. Front and back view of re-designed prototype are shown in Fig 5.1.

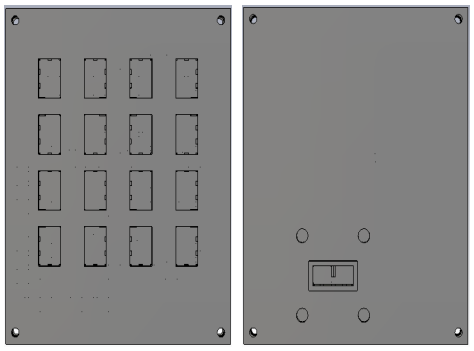

Figure 5.1: Front and back view of re-designed prototype.

As boundary condition used now are all open and the structure changed quite much, the performance of prototype changes as well. New results and parameters are shown below.

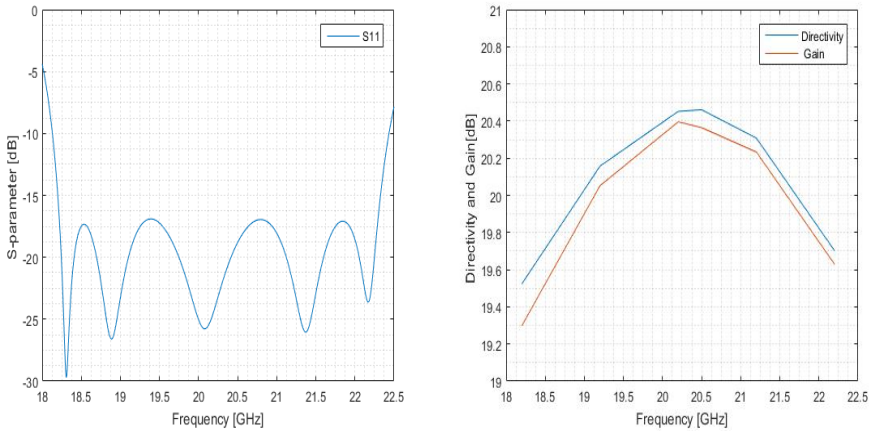

Figure 5.2: Simulated results of prototype re-designed.

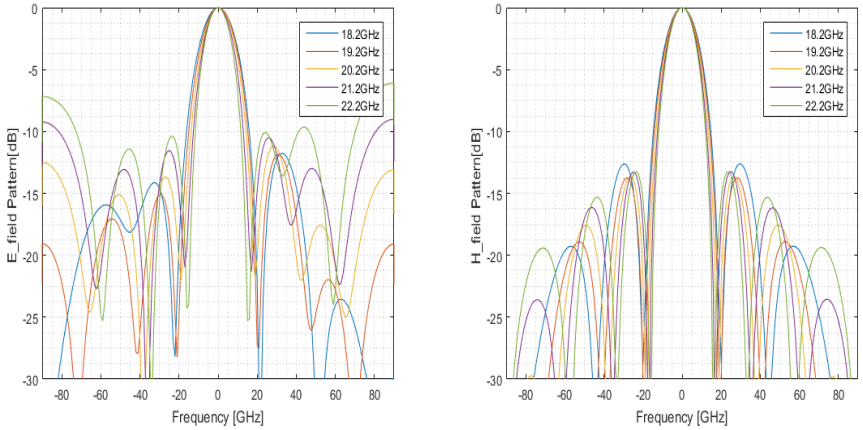

Figure 5.3: E-(left) and H-field(right) pattern of prototype re-designed.

Reason for dropping in directivity is due to the higher grating lobe level at high frequency.

Table 5.1: Values of 4×4 slot array.

Symbol	Description	*Value*
sl	length of slot	8.53mm
sw	width of slot	5.79mm
cpl	length of coupling slot	6.8mm
cpw	width of coupling slot	3.99mm
offset_ts	offset distance of T-section	0.76mm
tsl	length of T-section	5.62mm
tsw	width of T-section	2.88mm
xl	length of x-axis ridge	2.35mm
xw	width of x-axis ridge	3.94mm
yl	length of y-axis ridge	1.68mm
yw	width of y-axis ridge	1.61mm
a	width of ridge	2mm
c	dimensions of pin	1mm
d	height of pin and ridge	3.6mm
b_angle	angle of bend	437.65°
b_w	width of bend	2.648mm
L_probe	length of probe	2.656mm
W_probe	width of probe	1.06mm
Offset_trans	offset distance of WR-ridge transformer	0.7mm
L_trans	length of WR-ridge transformer	4.2mm
W_trans	width of WR-ridge transformer	3.21mm
L_transT1	length of first Tjunction transformer	4.3mm
W_transT1	width of first Tjunction transformer	2.85mm
L_transT2	length of second Tjunction transformer	6mm
W_transT2	width of second Tjunction transformer	3.47mm
W1	Width of first T-junction compensation bend	10mm
theta1	angle of first T-junction compensation bend	5.554°
W2	Width of second T-junction compensation bend	3.64mm
theta2	angle of second T-junction compensation bend	31.32°
ts	thickness of sub plane	10mm
tm	thickness of mid plane	1.32mm
tt	thickness of top plane	1mm
x	total length in x-axis	59mm
y	total length in y-axis	72mm

5.2 Testing

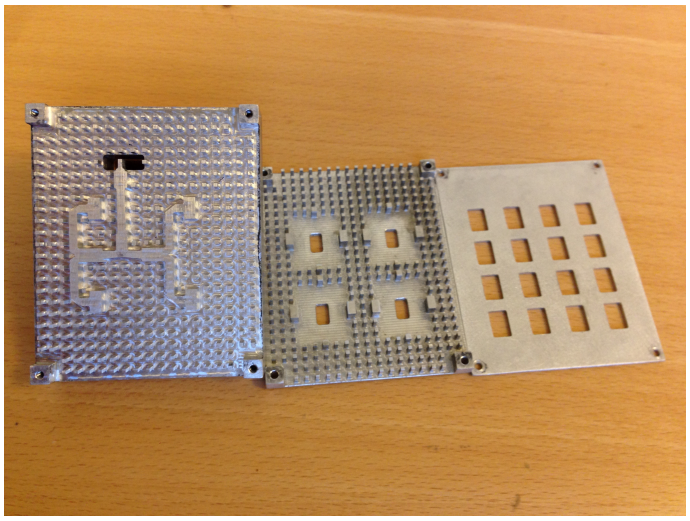

Figure 5.4: Manufactured Prototype.

The prototype is manufactured using Aluminium metal. In Fig 5.4, three planes of the prototype is shown. S-parameters are measured with vector network analyzer(VNA). Results are shown in Fig 5.5 together with simulated ones.

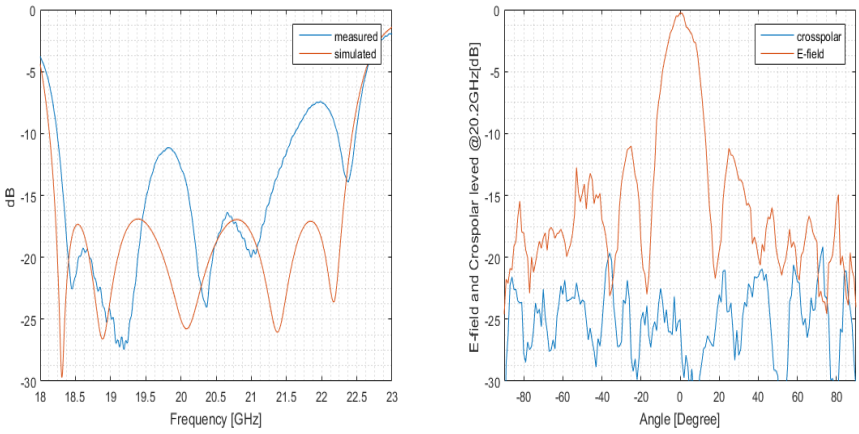

Figure 5.5: Simulated and tested results of prototype.

The measured S_{11} is in reasonable agreement with simulated value. The degradation in S_{11} is due to the tolerance in air gap between the different layers. Also, the waveguide adapter may have contribution in higher S_{11} level as the calibration was done up to VNA port only.

Radiation patterns are measured in anechoic chamber. E- and H-plane patterns are shown in Fig 5.6. Both E and H plane pattern agreed with simulations quite well at low frequency, but have discrepancies above 20GHz. The reason of the discrepancies

lie to the fact that the transmit antenna(Quad-ridge feed horn) does not work well above 20GHz. Also, the losses in the cables increase above 20GHz which lowers the overall dynamic range of the chamber.

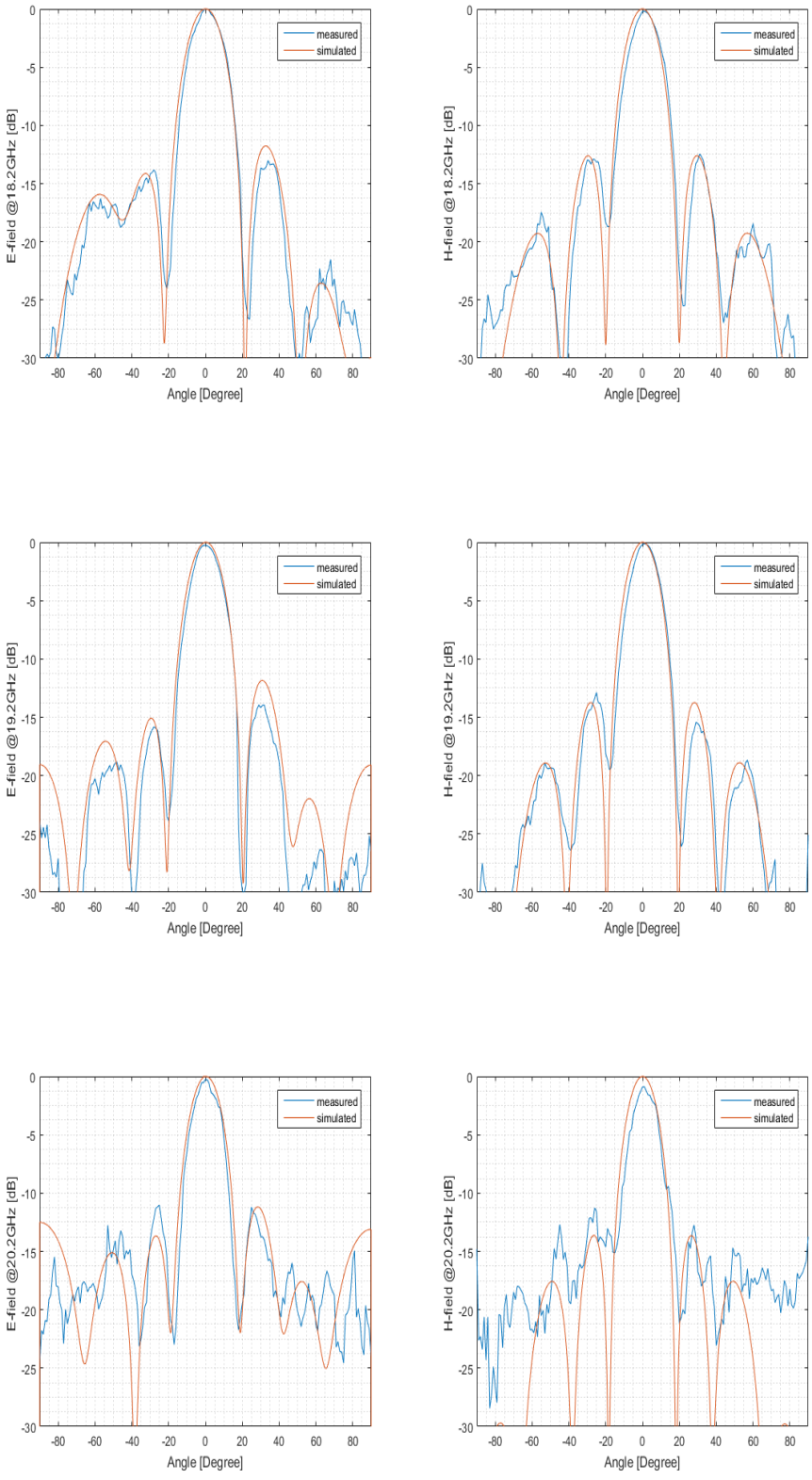

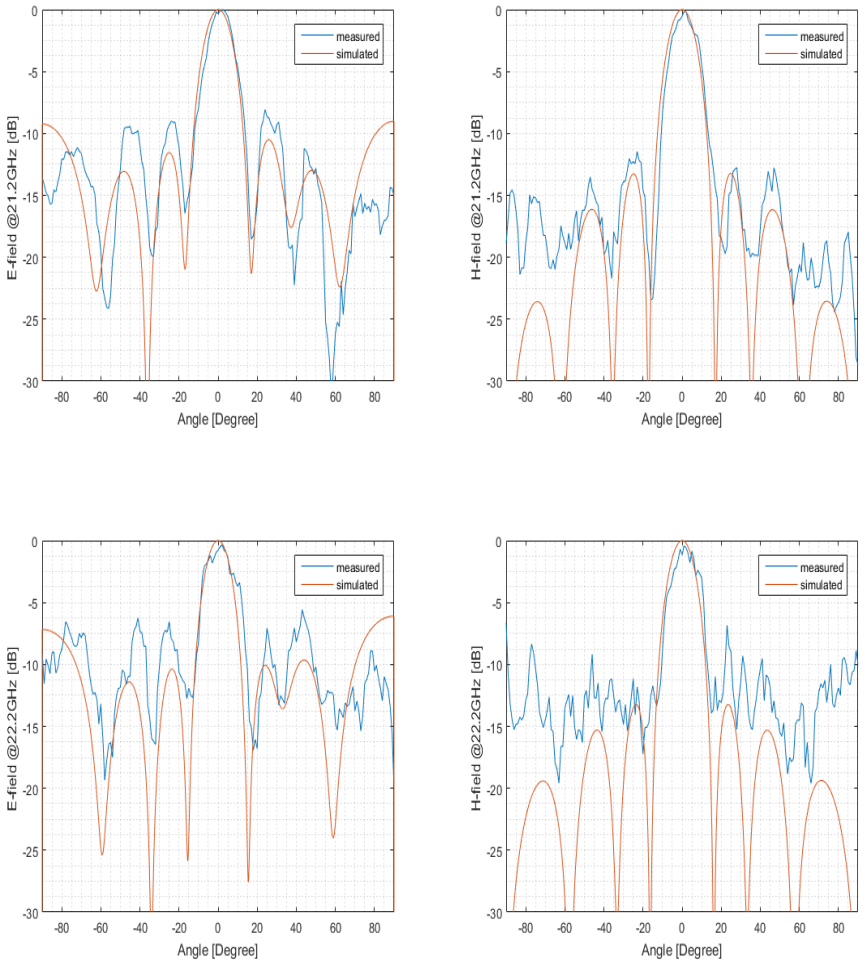

Figure 5.6: Simulated and tested radiation pattern in E- and H- plane.

6

Conclusion and Future Work

6.1 Conclusion

Initially, a unit cell with cavity at 20GHz is designed. Signal excited from bottom layer is coupled into four cavities, then it is transmitted through radiating slots. S_{11} is -15dB over a 20% relative bandwidth. And using factor scaling, another uni cell at 60GHz is designed, which has a relative bandwidth of 15% (57 to 66GHZ) with S_{11} of -20dB.

Then, a full corporate feed network is designed to feed slot array on upper layer. The simulated reflection loss is -25dB over the desired spectrum and quit smooth. Insertion loss is -0.1dB which is small enough to be neglected.

Finally, these two layers were combined together to build a double layer cavity backed slot array antenna. The prototype is manufactured and tested. Measured S_{11} remains below -11dB from 18GHz to 21GHz. Radiation patterns agree with simulation at low frequency, and over 21GHz there is discrepancies due to the dynamic range is limited by cable losses and transmit antenna's working range.

But still the prototype achieves a bandwidth of 15% with reasonably good radiation patterns taking into account the measurement accuracy of the anechoic chamber.

6.2 Future Work

Since the United States Federal Communications Commission(FCC) allocated a spectrum for license free between 57-66GHz and 120GHz in 2001 while agreed by other governments[29, 30], there will be a highly demand for devices at high frequencies[31, 32]. As in [33], gap waveguide working at 240GHz-320GHz has already been tested, its attenuation loss is comparable to metal waveguide and much less than planar transmission lines, just as shown in former chapters at K- and V-band.

The 60GHz unit cell designed in chapter four could be used to design 60GHz slot array antenna. And also, the 20GGHz unit cell can be a basic unit and scaled up to any frequency for future design usage at even higher frequencies.

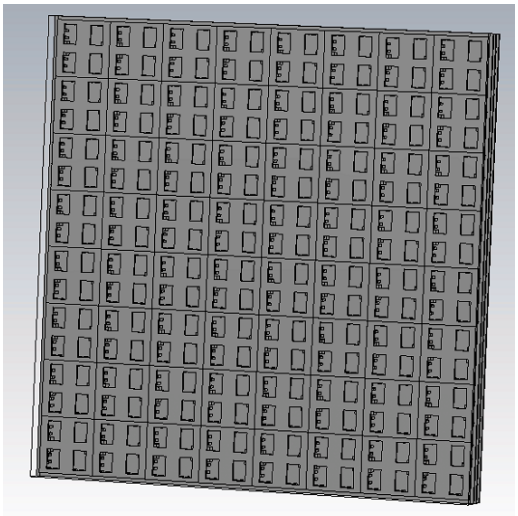

Figure 6.1: Schematic diagram of 60GHz 16×16 element array antenna.

Bibliography

[1] W. E. McKinzie and N. Alexopoulos, "Leakage losses for the dominant mode of conductor-backed coplanar waveguide," Microwave and Guided Wave Letters, IEEE, vol. 2, pp. 65-66, 1992

[2] M. Tsuji, H. Shigesawa, and A.A. Oliner, "Simultaneous Propagation of bound and leaky dominant modes on printed-circuit lines," IEEE Trans. Microw. Theory and Tech., vol. 43, no. 12, pp. 3007-3019, Dec. 1995.

[3] Ken Kuang, Franklin Kim, Sean S. Cahill,'RF and Microwave Microelectronics Packaging',Spring Science + Business Media,2010,ISBN 978-1441909831

[4] Lamminen, A.; Saily, J.; Vimpari, A.R.; "60-GHz Patch Antennas and Arrays on LTCC With Embedded-Cavity Substrates," Antennas and Propagation, IEEE Transactions on , vol.56, no.9, pp.2865- 2874, Sept. 2008

[5] Shang,X.; Ke, M ; Wang, Y.; Lancaster, M.J., "Micro machined W-band waveguide and filter with two embedded H-plane bends," in Microwaves, Antennas and Propagation, IET , vol.5, no.3, pp.334-339, Feb. 21 2011

[6] Becker, J.P.; East, J.R.; Katehi, L.P.B., "Performance of silicon micromachined waveguide at W-band," in Electronics Letters , vol.38, no.13, pp.638-639, 20 Jun 2002

[7] Guan-Long Huang; Shi-Gang Zhou; Tan-Huat Chio; Hon-Tat Hui; Tat-Soon Yeo, "A Low Profile and Low Sidelobe Wideband Slot Antenna Array Feb by an Amplitude-Tapering Waveguide Feed-Network," in Antennas and Propagation, IEEE Transactions on, vol.63, no.1, pp.419-423, Jan. 2015

[8] Y.Miura, J.Hirokawa, M.Ando, Y.Shibuya and G.Yoshida, "Double-layer full-corporate-feed hollow-waveguide slot array antenna in the 60GHz-band," IEEE Trans. Antennas Propagate., vol.59, no.8, pp.1521-1527, Aug. 2011

[9] Zhou, S.; huang, g.; tanhuat, c.; Wei, G.; Yang, J., "Design of A Wideband Dual-Polarization Full-Corporate Waveguide Feed Antenna Array," in Antennas and Propagation, IEEE Transactions on., vol.PP, no.99, pp.1-1

[10] A. Uz Zaman, P.-S. Kildal, M. Ferndahl and A. kishk, “Validation of Ridge Gap waveguide Performance by Using In-house TRL Calibration Kit,”4th European Conference on Antennas and Propagation, Barcelona , April, 2010

[11] Elena Pucci, Ashraf Uz Zaman, Eva Rajo-Iglesias, Per-Simon Kildal, and Ahmed Kishk, “Study of Q—factors of ridge and groove gap waveguide resonators,” IET Microwaves, Antennas and Propagation, vol.7, iss.11, pp. 900-908, August 2013.

[12] Valero-Nogueira, E. Alfonso, J. I. Herranz, and P. S. Kildal, "Experimental Demonstration of Local Quasi-TEM Gap Modes in Single-Hard-Wall Waveguides," Microwave and and groove gap waveguide resonators," Microwaves, Antennas and Propagation, IET, vol. 7, pp. 900-908, 2013.

[13] Pucci, E.; Zaman, A.U.; Rajo-Iglesias, E.; Kildal, P.-S.; Kishk, A., "Losses in ridge gap waveguide compared with rectangular waveguides and microstrip transmission lines," in Antennas and Propagation (EuCAP), 2010 Proceedings of the Fourth European Conference on, vol., no., pp.1-4, 12-16 April 2010

[14] Kildal, P.-S., Alfonso, E., Valero-Nogueira, A., Rajo-Iglesias, E.: ‘Local metamaterial-based waveguides in gaps between parallel metal plates’, IEEE Antennas Wirel. Propag. Lett., 2009, 8, pp. 84–87

[15] Alfonso, E., Kildal, P., Valero, A., Herranz, J.I.: ‘Numerical analysis of a metamaterial-based ridge gap waveguide with a bed of nails as parallel-plate mode killer’. European Conf. Antennas and Propagation (EuCAP 2009), Berlin, Germany, 2009

[16] Kildal, P.-S.: ‘Three metamaterial-based gap waveguides between parallel metal plates for mm/submm waves’. European Conf. Antennas and Propagation (EuCAP 2009), Berlin, Germany, 2009 3

[17] Dr. Ashraf Uz Zaman ; Per-Simon Kidal,’gap waveguide in Handbook of Antenna Technologies’, Springer Science+Business Media Singapore 2015

[18] A. Kishk, A. Uz Zaman, and P.-S. Kildal, "Numerical Prepackaging with PMC lid - Efficient and Simple Design Procedure for Microstrip Circuits including the Packaging," ACES Applied Computational Society journal, vol. 27, no.5, pp. 389-398, May 2012

[19] A. U. Zaman, M. Alexanderson, T. Vukusic, and P. S. Kildal, "Gap Waveguide PMC Packaging for Improved Isolation of Circuit Components in High-Frequency Microwave Modules," Components, Packaging and Manufacturing Technology, IEEE Transactions on, vol. 4, pp. 16-25, 2014.

[20] E. Rajo-Iglesias, P. S. Kildal, A. U. Zaman, and A. Kishk, "Bed of Springs for Packaging of Microstrip Circuits in the Microwave Frequency Range," Components, Packaging and Manufacturing Technology, IEEE Transactions on, vol. 2, pp. 1623-1628, 2012.

[21] Rezaee, M.; Zaman, A.U.; Kildal, P.-S., "V-band groove gap waveguide diplexer," in Antennas and Propagation (EuCAP), 2015 9th European Conference on , vol., no., pp.1-4, 13-17 April 2015

[22] E. A. Alós, A. U. Zaman and P. S. Kildal, "Ka-Band Gap Waveguide Coupled-Resonator Filter for Radio Link Diplexer Application," in IEEE Transactions on Components, Packaging and Manufacturing Technology, vol. 3, no. 5, pp. 870-879, May 2013.

[23] Uz Zaman, A.; Kildal, P., "Ku band linear slot-array in ridge gapwaveguide technology," in Antennas and Propagation (EuCAP), 2013 7th European Conference on, vol., no., pp.3078-3081, 8-12 April 2013

[24] Zaman, A.U.; Kildal, P.-S.; Kishk, A.A., "Narrow-Band Microwave Filter Using High-Q Groove Gap Waveguide Resonators With Manufacturing Flexibility and No Sidewalls," in Components, Packaging and Manufacturing Technology, IEEE Transactions on, vol.2, no.11, pp.1882-1889, Nov. 2012

[25] E. Rajo-Iglesias and P.-S. Kildal, “Numerical studies of bandwidth of parallel plate cut-o realized by bed of nails, corrugations and mushroom- type EBG for use in gap waveguides", IET Microw. Antennas Propag., vol. 5, pp. 282-289, Mar. 2011.

[26] Raza, H.; Jian Yang; Kildal, P.-S.; Alfonso, E., "Resemblance between gap waveguides and hollow waveguides," in Microwaves, Antennas and Propagation, IET, vol.7, no.15, pp.1221-1227, December 10 2013

[27] Hopfer, S., "The Design of Ridged Waveguides," in Microwave Theory and Techniques, IRE Transactions on, vol.3, no.5, pp.20-29, October 1955

[28] A. U. Zaman and P. S. Kildal, "Slot antenna in ridge gap waveguide technology," in Antennas and Propagation (EUCAP), 2012 6th European Conference on, 2012, pp. 3243-3244.

[29] C. H. Park and T. S. Rappaport, “Short-range wireless communications for next- generation networks: UWB, 60 GHz millimeter wave PAN, and Zigbee,” IEEE Wireless Commun. Mag., vol. 14, no. 4, pp. 70–78, Aug. 2007.

[30] R. C. Daniels and R. W. Heath, Jr., “60 GHz wireless communications: Emerging requirements and design recommendations,” IEEE Veh. Technol.

Mag., vol. 2, no. 3, pp. 41–50, Sept. 2007.

[31] R. Merritt, B60 GHz groups face off in Beijing over Wi-Fi's future, EE Times, May 18, 2010, accessed on May 31, 2010.

[32] T.S. Rappaport, J.N.Murdock, F. Gutierrez, Jr., "State-of-the-art in 60 GHz Integrated Circuits and Systems for Wireless Communications," Proceedings of the IEEE„ August 2011, Vol. 99, No. 8, pp 1390-1436.

[33] S Rahiminejad, AU Zaman, E Pucci, H Raza, V Vassilev, S Haasl, P. Enoksson and P.-S Kildal, "Micromachined ridge gap waveguide and resonator for millimeter-wave applications," Sensors and Actuators A: Physical 186, 264-269.